Politecnico di Torino

Politecnico di Torino

Masters in Engineering and Management
A.a. 2023/2024

Modelling of thermophysical properties of eye cornea for cross-linking surgery analysis

Relatori:
Prof. Umberto Lucia
Dr. Giulia Grisolia
Dott. MariaRosa Astori

Candidati:
Sana Ahmad
S305973

List of Figures

Table of Contents

1. INTRODUCTION

1.1 General Anatomy

The eye is a complex sensory organ specialized for gathering visual information. The human eye is a specialized extension of the brain and the two are connected via the optic nerve. Each eyeball (human eye) is located in the anterior orbit, surrounded by a fibrous globe. The orbit or eye socket is a cone-shaped bony cavity which protects the eye. The socket is padded with fatty tissue, allowing the eye to move easily.

This orbital fat together with the connective tissues and extraocular muscles can be considered a supporting framework for the eyeball. In life, it is soft, incompressible, and limited in displacement by the fibrous strands, bands and ligaments which penetrate it. Human eyes are roughly spherical, filled with a transparent gel-like substance called the vitreous humour, with a focusing lens and an iris which regulates the intensity of the light, entering the eye, see Figure 1.1. In humans, the eye works by projecting images onto a light-sensitive retina, where the light is detected and signals are transmitted to the brain via the optic nerve. Light enters the eye from an external medium such as air or water, passes through the cornea, into the aqueous humour and is refracted by the lens. The lens inverts it and projects an image onto the retina, whose photosensitive cells trigger nerve impulses which travel to the brain. The crystalline lens and the cornea represent the main focusing system of the human eye. The cornea gives a larger contribution (about 2/3) to the total refraction than the lens, but whereas the curvature of the lens can be adjusted to "tune" the focus, the curvature of the cornea is fixed. This variable lens contribution is called accommodation and arises both from controlled changes in curvature and thickness along the lens's polar axis, mediated by ciliary muscle contractions.

The eyeball consists of three concentric layers or tunics, whose names reflect their basic functions: a fibrous tunic, consisting of the sclera behind and the cornea in front; a vascular pigmented tunic, comprising the choroid, ciliary body, and iris; and a nervous tunic, the retina, see Figure 1.1.

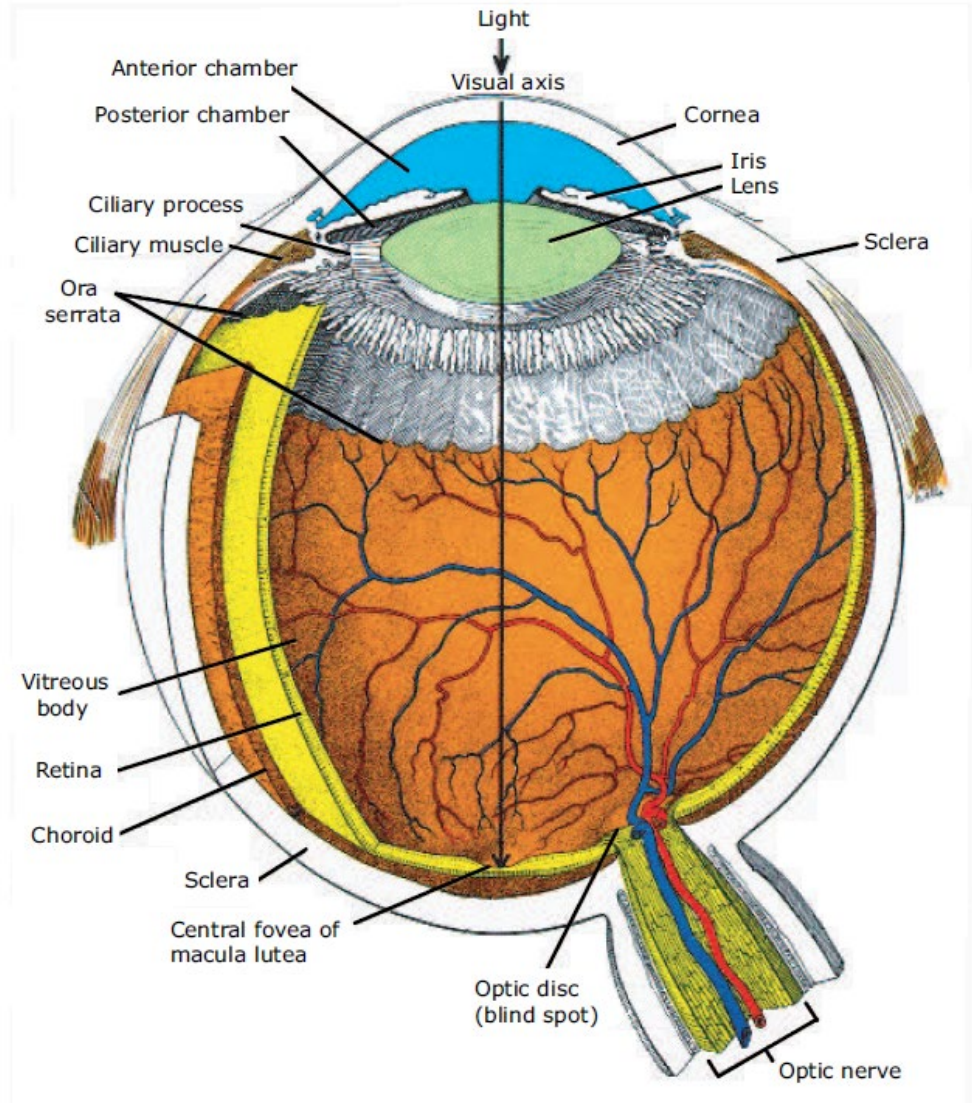

Figure 1.1: Schematic diagram of the human eye [1]

The cornea is a vital protective layer of our eye. It's part of the focusing process that helps to see clearly and keeps out things that don't belong in our eyes. They're also incredibly sensitive, helping us instinctively and immediately react to stop anything from harming our eyes further. Cornea is the clear, dome-shaped covering at the front of each of our eyes. It's like our eye's version of a windshield. It keeps debris, germs and more out. Its specific shape plays a key role in how our eyesight works and filters some ultraviolet (UV) rays.

The corneas are just in front of a fluid-filled chamber of our eye called the anterior (forward) chamber, which contains the aqueous humour. Behind the anterior chamber are our iris and pupil, followed by the lens as shown in the Figure 1.1. Surrounding our cornea is the sclera (the white part of our eye).

Because corneas are the first line of defence for the surface of your eye, they're also prone to injuries and damage. Fortunately, the corneas also have fast, effective self-repair abilities. The human cornea is transparent and plays a crucial role in vision by refracting light onto the retina. The cornea must refract light, contain the intraocular pressure (IOP) and provide a protective interface with the environment. Each of these functions is provided by a highly specialized substructural organization, and in absence of vessels.

The human cornea has six layers. They are;

Epithelium: The epithelium is the layer that covers the surface of the cornea. It is about 5-6 cell layers thick and filled with tiny nerve endings. That makes cornea indeed one of the most sensitive tissues of the body and this sensitivity serves a protective function. This is the outermost layer of the cornea. It's a physical barrier between the inside of our eye and the outside world, and it's incredibly sensitive to pain. Researchers estimate the cornea has about 300 to 600 times as many pain receptors as our skin. That sensitivity is protective. It makes us react strongly to stop or remove whatever's hurting our eyes. The epithelium blocks the passage of dust and germs and provides a smooth surface that absorbs oxygen and cell nutrients from tears, and then distributes these nutrients to the rest of the cornea. The basement membrane is the part where the epithelial cells anchor and organize.

Bowman's layer: This is a tough layer made mostly of collagen. It's there to provide structure and help our cornea hold its shape. Bowman's membrane, or anterior limiting lamina, lies directly below the basement membrane of the epithelium, has a thickness 8-12μm and is composed of randomly oriented collagen fibrils. The difficult access to Bowman's membrane protects the cornea from injury. But once injured, it resiliently regenerates, leaving a scar when the injury is deeper. The scar becomes opaque areas, causing the cornea to lose its clarity.

Stroma: This is the thickest layer of our cornea. It strengthens our cornea structure and helps bend (refract) light and focus it onto our retinas. The layer is dominating the mechanical response of the cornea to injury and accounting for 90% of its thickness. On a weight basis, the stroma is approximately 78% water, 15% collagen and 7% non-collagenous proteins, proteoglycans and salts.

Pre-Descemet's layer (PDL): Another name for this is "Dua's layer." Research indicates it's airtight, which means it's a very strong barrier separating the fluid inside our eye and the air from the outside world.

Descemet's layer: This layer is thin and stretchy but also remarkably strong. It's important to our eye structure and helps protect the inside of our eye from injury and infection. Descemet's membrane is strong sheet of tissue, which has similar mechanical properties as the lens capsule; both represent thick ocular basement membranes with a gradually increasing thickness with age. Descemet's membrane plays an important role in corneal hydration and the maintenance of the endothelium after wounding and surgery, regenerating readily after injury. Considering its thickness (~ 10 μm) and unique composition, it may be speculated whether Descemet's layer has a specialized function, beside the function as a basement membrane, that could be in mechanical support, filtration or liquid barrier.

Endothelium: This layer is mainly responsible for fluid balance in our cornea and the inside of our eye. It helps make sure there's just enough water and fluid in the stroma for our cornea to work as it should. The endothelium is the extremely thin, innermost layer of the cornea. Endothelial cells are essential in keeping the cornea clear. It pumps this excess fluid out of the stroma, which has the danger of swelling with water. Once endothelium cells are destroyed by disease or trauma, they do not recover. When a cell is lost, the others enlarge to fill up the gap. Too much damage to endothelial cells can lead to corneal oedema (swelling caused by excess fluid) and blindness, with corneal transplantation the only available therapy. An outline of layers of cornea is shown in the Figure 1.2.

Each layer has a specific job, but our cornea's true strength comes from how the layers work together. The layers work like laminate glass (also known as "safety glass") in car windshields. Laminate glass is two layers of glass with a sheet of thin, clear plastic between them. The plastic layer makes the whole piece much stronger (and sometimes, there are additional alternating glass and plastic layers to make it even stronger).

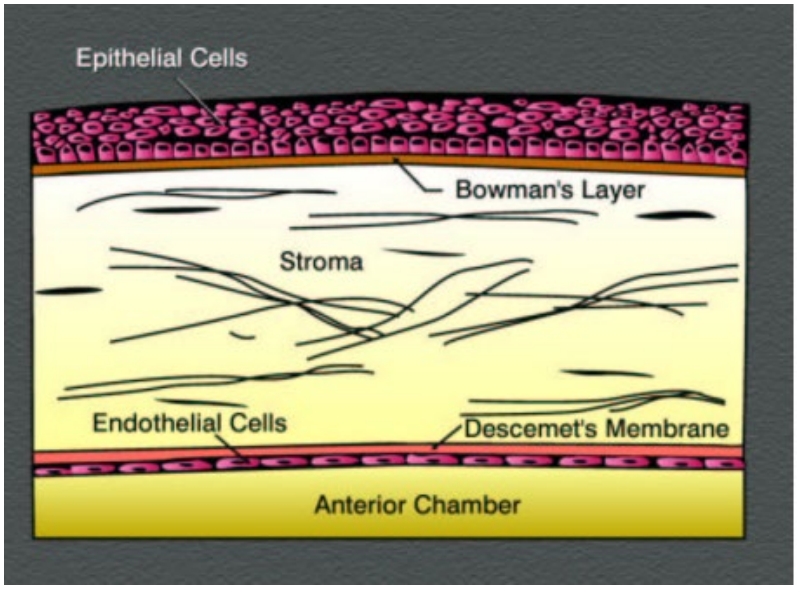

Figure 1.2: Layers of the Cornea [2]

The main function of the cornea is optical; it contributes to the total refractive eye power, accounting for about 80% of it. Refractive requirements are met by the regular anterior curvature of the cornea and the optically smooth quality of the overlying tear film. The resistance of the cornea is mainly due to its collagenous components. Collagen gives the cornea its strength, elasticity and form. It accounts for about 70% of the total dry mass of the cornea, the majority in fibrillar form. The collagen's unique arrangement and spacing are essential in producing the cornea's light-conducting transparency.

1.2 Corneal cross-linking (CXL)

Corneal cross-linking (CXL) surgery stands as a groundbreaking advancement in ophthalmology, revolutionizing the treatment of keratoconus and corneal ectasia. This innovative procedure, aimed at halting the progression of these conditions, offers hope and improved quality of life for countless individuals worldwide. Keratoconus and corneal ectasia are characterized by a weakening and thinning of the cornea, resulting in a conical shape and visual distortions. Traditional treatments, such as contact lenses or corneal transplants, may address symptoms but fail to prevent disease progression. In contrast, CXL surgery addresses the underlying biomechanical instability of the cornea, aiming to stabilize and strengthen it.

During CXL surgery, the patient's cornea is saturated with riboflavin (vitamin B2) eye drops, which are then activated by ultraviolet (UV) light. This combination induces chemical bonds

between collagen fibres in the cornea, increasing its rigidity and stability. The entire procedure is typically performed in an outpatient setting and takes about an hour.

Research has shown that CXL surgery effectively halts the progression of keratoconus and corneal ectasia in the majority of cases. By strengthening the cornea, it reduces the need for additional interventions such as corneal transplants. Moreover, CXL is associated with minimal risk and high patient satisfaction rates, making it a preferred choice for many individuals seeking long-term management of these conditions.

Here are some key thermophysical properties and considerations relevant to corneal cross-linking surgery:

Temperature: During the procedure, an ultraviolet (UV) light source is used to activate riboflavin (vitamin B2) eye drops that have been applied to the cornea. The temperature of the cornea may increase slightly due to UV light exposure, but it's generally well-controlled to prevent damage to the surrounding eye tissues.

UV Absorption: Riboflavin is applied to the cornea to enhance its UV absorption, making the cross-linking process more effective. The UV light activates riboflavin molecules, which then create chemical bonds within the corneal collagen fibres.

Optical Properties: The cornea is a transparent tissue with unique optical properties, and the goal of CXL is to maintain its transparency while strengthening it. The absorption and scattering of light within the cornea are important factors in preserving visual acuity and preventing complications.

Thermal Conductivity: The thermal conductivity of the cornea is essential to consider during the procedure to prevent overheating or thermal damage. The UV light source used for cross-linking must be carefully controlled to avoid excessive heat generation.

Biomechanical Properties: One of the main objectives of CXL is to increase the cornea's biomechanical stability. This is achieved by forming additional covalent bonds between collagen fibres in the cornea. The thermophysical properties are crucial in ensuring the strengthening effect is achieved without compromising the cornea's structural integrity.

Water Content: The cornea contains a significant amount of water, which plays a role in its thermophysical properties. Water content affects how the cornea responds to UV light and the formation of cross-links within the collagen fibres.

Refractive Index: The refractive index of the cornea is important for maintaining proper vision. Any changes in the corneal thermophysical properties should not adversely affect its refractive properties.

During corneal cross-linking surgery, a delicate balance must be maintained to achieve the desired strengthening effect while minimizing potential side effects or damage to the cornea. Specialized equipment, eye protection, and precise control of the UV exposure are used to ensure the procedure's success and the preservation of vision.

1.3 Temperature during CXL

Proper temperature control is crucial to ensure the safety and effectiveness of the cross-linking surgery. Here are the key effects of temperature in CXL surgery:

Riboflavin Activation: Riboflavin, a photosensitizing agent, is applied to the cornea during CXL. It is then activated by ultraviolet (UV) light. Temperature influences the rate of riboflavin activation. A controlled temperature increase can enhance the efficiency of this activation process, leading to more effective cross-linking of corneal collagen fibres.

Thermal Damage Prevention: Excessive heat can potentially damage the cornea and surrounding ocular tissues. It's critical to maintain proper control of temperature to prevent thermal damage, which could compromise the success of the procedure or lead to unwanted side effects.

Optimal Cross-Link Formation: Temperature affects the chemical reactions that lead to the formation of additional covalent bonds within the corneal collagen fibres. Maintaining the right temperature range helps ensure that the cross-linking process is effective in enhancing the biomechanical stability of the cornea.

Patient Comfort: Elevated temperatures within the eye can cause discomfort and distress to the patient. Proper temperature control ensures that patients experience minimal discomfort during the procedure, contributing to a smoother surgical experience.

Corneal Hydration: Temperature can influence the hydration status of the cornea. During CXL, there may be a temporary decrease in corneal hydration. This dehydration can affect the cross-linking process and the mechanical properties of the cornea.

Equipment Cooling: The UV light source used for CXL generates heat. Adequate cooling mechanisms are in place to control the temperature of the equipment and maintain a stable temperature environment during the procedure.

Heating Effects: The UV light source is carefully controlled to avoid overheating of the cornea. Precise exposure parameters are determined to ensure that the temperature increase remains within safe limits to prevent any thermal damage to the cornea.

In CXL surgery, it is crucial to strike a balance to take advantage of the positive effects of temperature on riboflavin activation and cross-link formation while preventing the adverse effects of excessive heat. Ophthalmologists and corneal specialists are trained to carefully control and monitor temperature during the procedure to achieve the desired therapeutic effects while ensuring patient safety.

Modelling the temperature distribution in the cornea during cross-linking surgery can be complex but is crucial for ensuring the safety and efficacy of the procedure. The primary goal is to prevent thermal damage to the cornea while still achieving the desired strengthening effect. Several factors influence the temperature distribution in the cornea during cross-linking surgery:

UV Light Source Parameters: The primary heat source in CXL surgery is the UV light source used to activate riboflavin. Modelling the UV light source's intensity, wavelength, and exposure time is essential. These parameters determine the amount of energy delivered to the cornea and influence the temperature rise.

Riboflavin Distribution: The distribution of riboflavin in the cornea affects how it absorbs UV light and contributes to temperature increase. Modelling the diffusion of riboflavin in the cornea is essential.

Corneal Thickness: The thickness of the cornea plays a role in temperature distribution. A thinner cornea may experience greater temperature increases than a thicker one due to differences in heat dissipation.

Thermal Properties: The thermal properties of the cornea, such as thermal conductivity and specific heat capacity, are critical parameters for modelling temperature distribution. These properties affect how heat is conducted and stored within the tissue.

Heat Dissipation: The cornea is well-vascularized and has mechanisms for heat dissipation. Modelling the heat dissipation mechanisms, such as heat conduction into adjacent tissues and heat transport through the tear film, is important.

Duration of UV Exposure: The duration of UV exposure significantly impacts the temperature increase in the cornea. Prolonged exposure can lead to higher temperatures.

Tissue Absorption and Scattering: The cornea's optical properties, including absorption and scattering coefficients, influence how UV light penetrates the tissue and contributes to temperature changes.

To model the temperature distribution in the cornea during cross-linking surgery, we can use mathematical and computational techniques. Finite element analysis (FEA) or computational fluid dynamics (CFD) simulations can be employed to solve the heat transfer equations. These simulations consider heat generation from the UV source, heat conduction within the cornea, heat dissipation to surrounding tissues, and other relevant factors. Advanced software tools and numerical methods can help simulate and visualize temperature distributions within the cornea.

It's important to note that CXL procedures are typically guided by protocols and safety measures to control and monitor the temperature to prevent thermal damage. Patient-specific considerations, including corneal thickness and hydration, are also taken into account. Modelling can aid in optimizing and refining the procedure for each patient's unique circumstances. However, any modelling must be validated against clinical data to ensure its accuracy and safety. This work should be conducted by experienced professionals and researchers in collaboration with ophthalmologists and engineers with expertise in modelling and simulation.

1.4 Refractive Index

The refractive index of the cornea is an important factor to consider in corneal cross-linking (CXL) surgery, as it can influence the optical properties and visual outcomes. Here are some of the effects and considerations of the refractive index in CXL surgery:

Preservation of Refractive Properties: One of the primary goals of CXL surgery is to strengthen the cornea while preserving its optical properties, including its refractive index. Alterations to the refractive index can affect visual acuity and the patient's ability to focus properly. Therefore, maintaining the refractive properties of the cornea is crucial during the procedure.

Monitoring Optical Changes: Ophthalmologists and surgeons carefully monitor the patient's corneal shape and refractive status before, during, and after CXL surgery. This monitoring helps ensure that any changes in the refractive index do not negatively impact the patient's vision.

Postoperative Refractive Stability: CXL surgery is designed to halt the progression of conditions like keratoconus while preserving the patient's current refractive state. The refractive index should ideally remain stable postoperatively, and the procedure should not induce unwanted changes in visual correction.

Customization for Each Patient: The refractive index can vary among individuals due to differences in corneal anatomy, thickness, hydration, and other factors. CXL procedures may need to be customized to account for these individual variations to maintain proper vision.

Corneal Transparency: Changes in the refractive index should not compromise the cornea's transparency. The cornea is a transparent tissue, and maintaining its clarity is essential for good vision. Any opacity or changes in the refractive index that affect transparency can result in visual disturbances.

Combination with Other Procedures: In some cases, CXL may be combined with other refractive surgeries like PRK (Photorefractive Keratectomy) or LASIK (Laser-Assisted in Situ Keratomileusis). In such cases, the refractive index is a critical factor to consider, as it may influence the patient's postoperative refractive state.

Patient Expectations: Patients who undergo CXL often have specific refractive and visual expectations. The refractive index and corneal changes should align with these expectations, and patient education is essential in managing postoperative outcomes.

It's important to note that while CXL primarily focuses on strengthening the cornea, the refractive outcomes can vary depending on the patient, the severity of their condition, and the surgical approach. Patients should have a thorough preoperative consultation with their ophthalmologist to discuss the potential effects on their refractive status and to set appropriate expectations.

Overall, maintaining the refractive index and optical properties of the cornea as close to the preoperative state as possible is a key consideration in CXL surgery to ensure that the patient's vision is not negatively impacted while addressing the underlying corneal condition.

The cornea consists of three basic layers: the epithelium, the stroma and the endothelium. The stroma constitutes around 90% of the thickness of the cornea. The stromal lamellae, which are long, parallel, cylindrical collagen fibrils embedded in a ground substance whose refractive index is lower than that of the collagen fibrils. The normal cornea contains 76.2% water by weight. A constant corneal hydration is essential for the maintenance of its transparency. A swollen corneal stroma contains irregular regions in which refractive index fluctuations scatter light and cause the cornea to opacify. Changes in the corneal thickness are known to be proportional to changes in corneal hydration. Accurate measurement of the corneal hydration and thickness is useful for both diagnostic and monitoring purposes as well as surgical planning. For example, cornea thickness decreases with prolonged contact lens wear because of hypoxia. In excimer laser kerato refractive surgery, 53 μm of central stromal tissue in a 4 mm diameter area is removed to correct -10 diopters of myopia; accurate measurement of corneal thickness may improve.

A mathematical model of the relationship between the corneal refractive index and hydration was developed by Kim *et. al.* [3]. The refractive index of the cornea, n_{co}, is given by

$$n_{co} = n_{cf} \cdot f_{cf} + n_{gs} \cdot f_{gs}$$

where,

n_{cf} is the refractive index of the collagen fibrils,

n_{gs} is that of the ground substance,

f_{cf} is the volume fraction of the collagen fibrils

f_{gs} is that of the ground substance *(*$f_{cf} + f_{gs} = 1$*)*.

It is assumed that the drying of the cornea dehydrates only the ground substance so that the corneal refractive index increases without changing the water content of the collagen fibrils, in which water is tightly bound. When the ground substance is completely dehydrated, the corneal refractive index will be close to that of the collagen fibrils, because the volume fraction of the collagen fibrils and that of the dehydrated ground substance are found to be ~30% and ~10%, respectively. Similarly, the swelling of the cornea takes place only in the ground substance, keeping the hydration of the collagen fibrils constant. The volume fractions of the collagen fibrils and the ground substance are,

$$f_{cf} = \frac{V_{cf}}{V_{cf}+V_{gs}} \quad \text{and} \quad f_{gs} = \frac{V_{gs}}{V_{cf}+V_{gs}}$$

where V denotes the volume of each component. The volume fraction, $V_{cf,}$ and the refractive index, n_{cf}, of the collagen fibrils are constant over changes in the corneal hydration because the hydration takes place only in the ground substance. The ground substance is considered as a mixture of dry material and water. The volume of the ground substance, Vgs, is expressed by

$$V_{gs} = V_{0gs} + V_{H2O}$$

Where V_{0gs} is the volume of the ground substance when the ground substance is completely dehydrated and V_{H2O} is the water content of the ground substance.

The refractive index of the ground substance, n_{gs}, can be decomposed such that

$$n_{gs} = n_{0gs}\frac{V_{0gs}}{V_{gs}} + n_{H2O}\frac{V_{H2O}}{V_{gs}}$$

where n_{0gs} is the refractive index of the dry ground substance and n_{H2O} is that of water. Then, V_{H2O} is given by the definition of the hydration

$$V_{H2o} = H\,(V_{0gs} + V_{cf})$$

where *H* is the corneal hydration. Substituting equations (7)–(10) into (6), equation (6) is rewritten as a function of *H*

$$n_{co}(H) = n_{H2O} + \frac{V_{cf}\left(n_{cf} - n_{cf}\right) + V_{0gs}\left(n_{0gs} - n_{H20}\right)}{(H + 1)\left(V_{0gs} + V_{cf}\right)}$$

$$= a + \frac{b}{H+1}$$

where *a* and *b* are constants

The corneal hydration, which is defined by the ratio of the water weight to the completely dry weight of the cornea was calculated from the known linear relationship between bovine corneal hydration and thickness

$$H = 5.3 \times 10^{-3}\,T - 0.67$$

where H is the hydration of the corneal stroma and T is the thickness of the corneal stroma in μm.

Using the above equation, the corneal refractive index can be expressed as a function of T

$$n_{co}(T) = a + \frac{b}{\mathbf{5.3 \times 10^{-3}}\,\mathrm{T}+0.33}$$

1.5 Intraocular pressure (IOP)

The fluid pressure inside an eye is called the intraocular pressure (IOP). It is a key diagnostic parameter to determine the health of the eye. In clinical practice, a tonometry test is employed for the IOP measurement, which is done through the corneoscleral coat by different types of tonometers. Tonometry is a part of routine eye examinations to screen for increased IOP and assess glaucoma risk and treatment efficacy.

To use a thermodynamic approach to the analysis of the cross-linking effect on eye pressure, it is considered that the flows related to the IOP are water inflows and outflows between the ocular anterior chamber and blood vessels. Therefore, considering the eye as an open system of the body, apply the first law of thermodynamics [4]

$$\dot{Q} - \dot{W} = \frac{d}{dt}\left[U + p_0 V + \int_V \rho\left(e_k + e_p\right) dV\right]_{CV} + \dot{m}_{out}\left(h + e_k + e_p\right)_{out} - \dot{m}_{in}\left(h + e_k + e_p\right)_{in} \quad (1)$$

where Q is the heat power exchanged between the cornea and its external environment, W is the mechanical power carried out by the tissue about the pressure and elastic properties of the cornea, U is the internal energy, p_0 is the external environmental pressure, V is the volume of the anterior chamber, ρ is the water density, e is the specific energy, k stands for kinetic, p as a subscript means potential, h is the specific enthalpy of the water, *in* means inflow, *out* means outflow, and CV means control volume. The kinetic energy and the potential energy are so small that they can be considered null; moreover, it has been analysed the behaviour of the eye during the time of observation, so that the time can be integrated, obtaining:

$$Q - W = (m_{out} - m_{in})c_v T_w + p_0 \Delta V + m_{out} c_p T_w - m_{in} c_p T_{in} \quad (2)$$

where c_v is the specific heat at a constant volume of the water inside the anterior chamber, c_p is the specific heat at a constant pressure of the water, T_w is the temperature inside the anterior chamber, T_{in} = 37◦C is the temperature of the inflow water, m_w is the mass of water, T_0 is the external environmental temperature, considered in the range [-30◦C, 40◦C], and ΔV is the volume variation due to water stagnation in the ocular anterior chamber. Then, considering that the anterior chamber exchanges heat with the environment by the cornea surface, we can write:

$$Q = -m_w c_v (T_w - T_0)$$

obtaining:

$$-W = (m_{out} - m_{in}) c_v T_w + p_0 \Delta V + m_{out} c_p T_w - m_{in} c_p T_{in} + m_w c_v (T_w - T_0) \quad (4)$$

Then, we can evaluate the work carried out by the water against the external surface of the anterior chamber as:

$$W = -V \cdot \Delta \text{IOP} \quad (5)$$

Now considering the extended Bernoulli's equation;

$$W = \int p dV - p_0 \Delta V - W_\lambda - \Delta E_k - \Delta E_p \quad (6)$$

where W_λ is the work lost for irreversibility, E_k is the kinetic energy and Ep is the cornea elastic potential energy, and introducing this last relation (6) into the relation (4), it follows that the elastic potential variation of the cornea results as:

$$\Delta E_p = (m_{out} - m_{in}) c_w T_w + m_{out} c_w T_w - m_{in} c_w T_{in} + m_w c_w (T_w - T_0) \quad (7)$$

Finally, considering the relation (7) and (6) it follows that

$$\Delta E_p = Y \cdot s = (2m_{out} - m_{in}) c_w \left(\frac{\Delta (V \cdot \text{IOP})}{c_w (2m_{out} - m_{in} + m_w)} + \frac{m_{in} T_{in} + m_w T_0}{2m_{out} - m_{in} + m_w} \right) - m_{in} c_w T_{in} + \\ + m_w c_w \left[\left(\frac{\Delta (V \cdot \text{IOP})}{c_w (2m_{out} - m_{in} + m_w)} + \frac{m_{in} T_{in} + m_w T_0}{2m_{out} - m_{in} + m_w} \right) - T_0 \right]$$

where Y is the coefficient of elasticity and s is the cornea thickness. The thermodynamic model introduced holds to the following statement: any variation in the cornea thickness holds to a variation of the eye pressure, and/or to the inner temperature. It is highlighted that the cross-linking therapy generates work on the cornea, with the result being able to modify the IOP and temperature, which represent a footprint of the surgery. The fundamental problem is whether this footprint is continuous in time or if the eye system will come back to the initial condition of IOP and temperature. It can be concluded that:

• The number of patients is limited because keratoconus is a rare disease, but this set of patients represents a first statistic sample of analysis about the thermal effect of the cross-linking therapy, so it allows us to evaluate the effectiveness of the model.

• The data confirm the theoretical model introduced; indeed, it allows us to state that IOP increases immediately after the cross-linking surgery, with a thermal memory to the eye system;

• This thermal memory, a sort of thermal hysteresis, in the eye system confirms the complex and non-linear physical answer of this biosystem about the thermal effect.

1.6 Central Corneal Thickness (CCT)

Central corneal thickness (CCT) appears to play an important role in the exact measurement of intraocular pressure and in the diagnostic assessment of glaucoma. Since corneal swelling pressure depends on IOP, corneal thinning is likely to appear with increased IOP, while decreased IOP tends to cause corneal thickening. The influence of these pressure-induced changes on the accuracy of application tonometry is unknown. However, the effect of the baseline corneal thickness on the accuracy of GAT (Goldmann-type applanation tonometers) has been studied quite intensively by Darja Ljubimova [5]. In manometric studies it was observed that thin corneas produce falsely low-pressure readings and thick corneas cause measured IOP to be too high, while GAT readings were accurate at CCT of 0.52 mm. In was also found that mean error induced by CCT varied with the IOP, being lower at low IOP and vice versa. At a true IOPT of 20 mmHg, it can be calculated a mean underestimation of 5.2 mm Hg that was given by applanation tonometry in eyes with CCT of 0.45 mm, and an overestimation of 4.7 mmHg that was found with CCT of 0.59 mm. This is a span of 9.9 mmHg in the tonometer reading for the same IOPT which corresponds to 0.71 mmHg change per 10 μm change in CCT. The overall conclusion from the studies is that IOP measurements using tonometry are affected by differences in CCT. Although the majority of the studies are based on the statistical analyses of clinical data, mathematical approaches as well as numerical modelling are also successfully used, producing results with a similar trend, where high CCT leads to IOP overestimation, and vice versa. Correlation between CCT and IOP is probably nonlinear. Corrections of Goldmann readings can be achieved in various ways when CCT variations are considered.

2. CORNEAL BIOMECHANICS

The exact mechanisms of CXL at the molecular level, i.e. the nature of crosslinks and their location in the corneal extracellular matrix, have not yet been fully understood. The corneal collagen crosslinking involves mainly carbonyl-based crosslinks that mainly occur within collagen molecules themselves and between collagen and proteoglycan core proteins. The strengthening effects of the CXL treatment have been commonly investigated by performing uni-axial tensile experiments. This is because the cornea has often been seen as an isotropic material in the literature. However, it is well known that the cornea has an inhomogeneous and anisotropic extracellular matrix composed of collagen fibrils that are uniformly organized in stacks of lamellae. Studies have shown that the tensile modulus of the cornea is orders of magnitudes greater than its shear and compressive moduli. No previous studies determined corneal viscoelastic shear properties of collagen crosslinked corneas using torsional rheometry. The stiffening effects of the CXL procedure on the shear properties of the cornea were reported and discussed as a function of the applied frequency and shear strain at different levels of compressive strain. The oscillatory shear tests were performed by Hamed and Md [6] using a DHR-2 rheometer. The oscillatory rheology is a commonly used technique for characterizing the viscous and elastic shear response of materials. In this experimental method, the samples are subjected to oscillatory displacement and resulting forces are measured using a force transducer. The shear strain γ and shear stress τ can be represented as

$$\gamma = \gamma_0 \exp(i(\omega t - \delta))$$

$$\tau = \tau_0 \exp(i\omega t)$$

where $\omega=2\pi f$ is the angular frequency, f is the ordinary frequency, δ is phase angle, t is time, and τ_0 and γ_0 are shear stress and strain magnitude, respectively. The complex shear modulus G* relates the shear stress to shear strain. The storage modulus G′, and loss modulus G″ can be written as:

$$G' = |G^*|\cos\delta$$
$$G'' = |G^*|\sin\delta$$

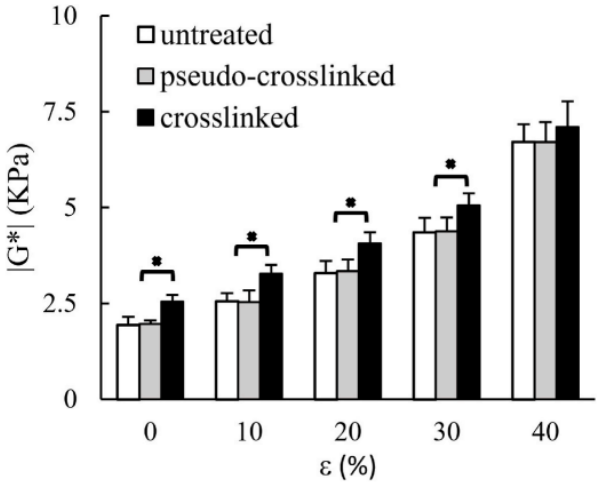

Figure 2.1: The effect of corneal collagen crosslinking on the complex shear modulus |G*|, averaged over the range of linear viscoelasticity, at different levels of compressive strain ε. [6]

No significant difference was observed between the shear response of pseudo-crosslinked and untreated samples; however, the crosslinking treatment significantly increased the magnitude of complex shear modulus when the compressive strain was less than 40% (no significant difference was observed at ε = 40%). The asterisk indicates significant differences between the two groups ($p<0.05$). The complex shear modulus of all samples increased significantly with increasing the compressive strain (no asterisk was shown for these groups so that the plot does not get crowded). The error bars indicate one standard deviation.

Material properties of the cornea affect the structural resistance of the shell, and, thus have an influence on measured IOP. Till recently, corneal biomechanical properties were not taken into account during GAT, assuming that IOP readings do not depend on them. The effect of corneal biomechanics on IOP measurement, and the interest in this effect has been enormous since popular refractive procedures for improving vision acuity represent different surgical manipulations with cornea structural integrity which led to changes in corneal shape and material characteristics. There have been reports of a reduction in IOP tonometric readings after PRK and LASIK. In some studies, no correlation between changes in pressure readings and changes in pachymetry or keratometry is found, which means that at least partly the reduction of IOP after surgery is due to modified biomechanical properties of the cornea. It is disputable, whether the true IOP changes after the refractive procedure. If this is not the case, incorrectly measured IOP may cause a delay in the recognition and treatment of possible glaucoma, resulting in ocular abnormalities. Hence an understanding of the biomechanical behaviour of the cornea has crucial importance for the development of predictive tools to aid clinical management of patients. Existing empirical surgical models do not explicitly identify

or account for the significant sources of biomechanical response in the postoperative visual outcome. Other applanation tonometers have been reported to be more useful than GAT in measuring IOP after refractive surgery.

The present study is of medical relevance since the failure to adjust IOPG estimates for variation in CCT or postoperative changes in the biomechanics of the human eyeball, influences clinical decision-making in an obvious way. A piece to that puzzle can be a mechanical model. Structural engineering analysis tools have been used to improve the understanding of the biomechanical behaviour of the cornea. This research is a collaboration between structural engineers and ophthalmologists. The initial study involved a vast literature survey on the behaviour of the cornea and corneoscleral envelope under different loads, constitutive governing laws, and material and geometrical properties. These data from a wide variety of sources have been drawn together to facilitate the construction of the two-dimensional finite element model of the cornea and three-dimensional model of the whole corneoscleral envelope. Consultations with ophthalmologists and clinicians were an important part of establishing the modelling procedures. It should be noted that procedures and assumptions used to specify the model are based entirely on what the author regards as sensible, reliable and reasonable interpretations of the available data. Numerical modelling is adopted as it has the potential to represent real-life conditions without having to adopt the simplifications necessary with mathematical closed-form solutions. Heterogeneous, orthotropic and nonlinear isotropic axisymmetric cornea models were constructed in two-dimension, whereas in three-dimension the human cornea was represented as a composite anisotropic structure with a layering pattern of collagen embedded in the ground substance.

2.1 General requirements for the numerical modelling

A finite element analysis is a valid tool in biomechanics when used correctly. A numerical study should obey several important demands before its predictions can be considered to have any clinical value. To achieve success in biomechanical research, the following conditions should be satisfied:

1. Model selection: - representation of the physical problem at hand to a sufficient degree of accuracy; - establishment of the detailed geometric model and suitable reference configuration; - assignment of material properties for all components of the modelled structure; - specification of the boundary conditions and operative forces;

2. FE formulation: - element consideration and solution methods;

3. Model verification: - estimation of the convergence tolerance, e.g. numerical accuracy; - proper identification of model parameters, (e.g. independence from the time or the repetition in the experiment used to derive them; association with measurable physical/physiological quantities);

4. Model validation: - ability to fit the experimental results; - sensitivity analysis of the results, consideration of the uncertainties in the model input parameters;

It should be noted in the present context that eyes from persons of the same age group exhibit variations in their mechanical and geometric characteristics. The differences in testing technique and health conditions of the donor's eyes produce a wide range of, sometimes, incommensurable and inconsistent bodies of measurements. When seeking general qualitative results, we need to assemble data from different sources and our modelling exercises lead to idealized models of a human eyeball. It bears emphasis that procedures and assumptions used to specify the model are based entirely on what the author regards as sensible, reliable and reasonable interpretations of the available data. It was necessary to choose some values for different parameters. All adopted assumptions and accepted choices are described in detail to allow the reader to judge their appropriateness, admissibility and validity

2.2 Two-Dimensional Modelling of Cornea

An axisymmetric FE nonlinear hyper elastic homogeneous and a linear elastic heterogeneous orthotropic model of the cornea have been constructed to investigate the influence of different corneal biomechanical parameters on the simulated GAT readings [5].

The model is two-dimensional and formulated in terms of axial symmetry with the axis of symmetry along the anterior-posterior axis of the eye. Because of the assumption about axis symmetry, we can greatly reduce the size of the computational model, since it is sufficient to model only half of the cross-section. The cornea was assumed to be a part of a composite spherical shell. Variation in thickness was considered for all the simulations developed. The thickness was minimum at the apex, Tc, increasing linearly along the meridional direction and achieving its maximum at the limbus, TL. Since one of the main goals was to investigate the effect of central corneal thickness (CCT) on GAT readings, Tc was varied within a certain range. In subsequent simulations, it is assumed that TL was always 0.150 mm larger than Tc as it was in Gullstrand’s No.1 schematic eye, in which Tc = 0.52 mm and TL = 0.67 mm. It is adopted the value of outside corneal radius equal to Rc = 7.8 mm and a base diameter equal to

D = 11 mm. The human corneal stroma exhibits a layered structure, comprising over 200 lamellae through its central thickness. Due to the large number of lamellar sheets through the thickness of the stroma, it is computationally intractable to model lamellae as individual components. Also adopted another approach, where corneal thickness was divided into five generalized lamellae or layers, from outer L1 to inner L5. Each of these layers had its own set of material properties, following Fernandez et al. (2005). By doing so, it also introduced the inhomogeneities in the stroma stiffness with depth variation. The tip of the applanation tonometer was 3.06 mm in diameter and modelled as an analytical rigid surface. Initially, the tonometer and cornea were separated from each other.

2.3 Material Properties

Due to the axial symmetry of the model, the anisotropic cornea could be approximated as an orthotropic or transversally isotropic material with principal axes in the meridian and circumferential directions. Since orthotropic constitutive laws in available software are only linear, the first model is linear elastic and heterogeneous. Stroma is divided into five layers and represents a part of the sphere. It has been introduced a local spherical coordinate system associated with the structure that depicts the principle material axis. The ground substance of the cornea is principally water, which characterizes the tissue as a nearly incompressible material. Considering this, it is reasonable to propose $\nu 23 = 0.5$, i.e. the tissue is incompressible in the membrane plane for circumferential stress. Linear elasticity in an orthotropic material is defined by giving the engineering constants: three elastic moduli E1, E2, E3; Poisson's ratios, $\nu 12$, $\nu 13$, $\nu 23$; and the shear moduli, G12, G13, and G23, associated with the material's principal directions. For simplicity, it is assumed that material was "nearly transversally isotropic" in plane $2 - 3$. It meant that Poisson's ratios and shear moduli obey the transversally isotropic law, but the elastic components are different. The reason we did not assume full transversal isotropy was an intention to simulate regional changes in the corneal material properties, as explained in more detail below. Also, due to the lack of experimental data and for the sake of simplicity, it is assumed that all stromal layers through the corneal thickness had equal Poisson's ratios, i.e. $\nu 12 = \nu 13$ and $\nu 21 = \nu 31$. According to mechanical laws, when the cornea is modelled as a thick shell, and accounting for the thickening at the periphery, the predicted meridional strains from the intraocular pressure loading should decrease from its maximum at the apex. This is inconsistent with experimental data since strain distribution on the anterior surface of the cornea is expected to be highly nonuniform. Based on experiments, observed that Simulations should be based on reasonable choices for the values of these

orthotropic parameters for each corneal layer. This is not trivial, since the cornea is highly heterogeneous in the central to peripheral and anterior to posterior dimensions, and the experimental corneal material data vary significantly, depending on the conditions of the experiments. First of all, it is already assumed ν23 = 0.5. There is a great dispersion of published data on Young's moduli, ranging from 0.005 to 10 MPa. It has been proposed baseline values for meridional elastic moduli at the corneal apex, E3i for 10% deformations, where i = (1; 5), i = layer number. In the simulations, we employ intraocular pressure loading, and 10% of strains seems to be quite large. The values of the corneal Young modulus reported for 1 − 3% strain levels were about 0.3 MPa. This value is close to the strains, occurring in the present type of simulations (IOP and GAT loading). It is the ground for the justification of the proposed assumptions. Moduli E2i identify the circumferential moduli for the cornea. Since it is proposed that corneal tissue was obeying "nearly transversally isotropic" law in the plane (2 − 3), and there has been no indication about the relationship between meridional and circumferential elastic moduli found in the literature, the difference in E2i and E3i was modelled to be small, in such a way, that E2i at the corneal center also fitted in the range of data reported.

2.4 Results

An example of the base and resulting configurations of the model after GAT is shown in Figure. After cornea inflation under full IOP, the model was subjected to the contact pressure from the analytical solid surface, until the contact area became 3.06 mm in diameter, representing a tonometer tip. At first, the cornea was loaded with a uniform pressure distribution, taken to be 0.002 MPa and 0.0028 MPa, which were equivalent to a pressure of either 15 or 21 mmHg. This preliminary step included physiological stresses which exist in all in vivo eyes. The initial stress-free shape of the corneas with different material descriptions was obtained by calibration and manually adjusted to fit the known in vivo geometry of the tissues. The final corneal stress distribution after GAT depends on the magnitude of the pre-stresses which appeared during the IOP-loading step. In turn, the stress distribution following the application of IOP relies on the tissue material description. Two main material models were considered: (1) – hyper elastic isotropic and (2) – elastic orthotropic models.

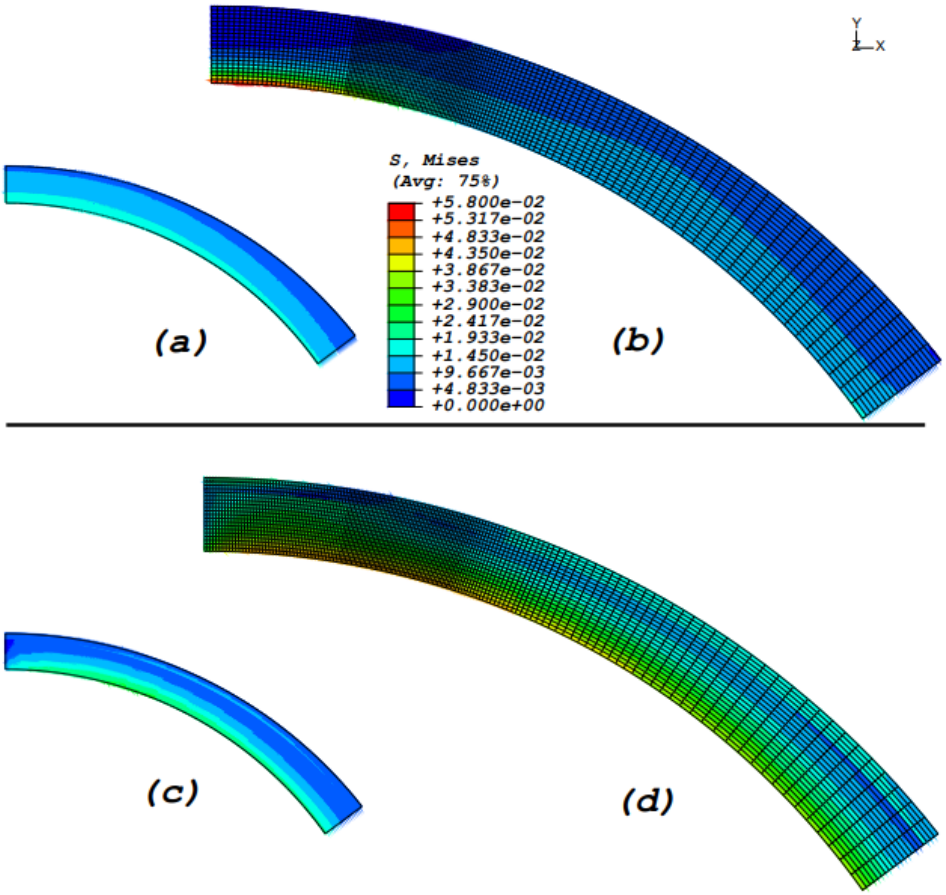

Figure 2.2: Stress distribution following full applanation under IOPT = 21mmHg. Contours are drawn on original undeformed geometries with in vivo geometric calibration parameters. Top figure shows hyper elastic isotropic model with material description based on data from Elsheikh & Anderson [7]: (a) – stresses due to IOP, (b) – stresses due to GAT; bottom figure shows elastic heterogeneous orthotropic model with material parameters from Table 2.1: (c) – stresses due to IOP, (d) – stresses due to GAT. Stress range: red=58 kPa, blue=0.0 kPa

Table 2.1: Material data for orthotropic elasticity at the corneal apex

Layer	E_1 (kPa)	E_2 (MPa)	E_3 (MPa)	ν_{23}	ν_{12}	G_{12} (kPa)	G_{23} (MPa)
L_1	6.2	0.522	0.622	0.5	0.01	124.4	0.9
L_2	2.8	0.175	0.275	0.5	0.01	55.0	0.9
L_3	2.8	0.179	0.279	0.5	0.01	55.8	0.9
L_4	3.0	0.204	0.304	0.5	0.01	60.8	0.9
L_5	3.3	0.231	0.331	0.5	0.01	66.2	0.9
Average	3.6	0.262	0.362	0.5	0.01	72.4	0.9

The applanation force required to fulfil GAT requirements for obtaining a 3.06 mm diameter of the contact region was measured; the corresponding applanated IOPG was calculated by dividing it to the contact area. The stress distributions recorded during different steps of simulation for both cases are shown in Figure 2.2. It was observed that increases in stresses

after the GAT procedure occurred near the tonometer contact area with limited effects elsewhere. Since changes in stresses were quite small at the periphery, it could be expected that boundary conditions at the limbus did not have a major influence on the model behaviour. In order to check this assumption additional simulations were performed. Similar results were observed for both orthotropic and hyper elastic models.

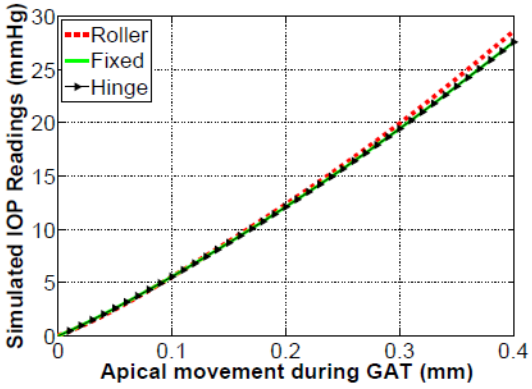

Figure 2.3: Comparison between hyper-elastic cornea models with material data from Elsheikh & Anderson [7] and different limbus boundary conditions.

The numerical estimation of the effect of limbus boundary conditions on IOPG measurements by nonlinear hyper elastic model with material data from Elsheikh & Anderson [7] is shown in Figure 2.3. It is evident that the boundary effect is not of major significance for the present model.

3. THREE-DIMENSIONAL MODELLING OF CORNEA

Cornea has a well-organized lamellar structure and can be considered as a material reinforced in one (in the limbus) or two (in the center) preferential directions, with the families of fibres distributed in a compliant ground substance. The remaining randomly distributed lamellae together with the corneal matrix define an underlying isotropic material. The collagen reinforcement can be modelled by means of rebar elements to incorporate anisotropy and the nonlinear behaviour. These rebars would represent generalised collagen fibres and are one-dimensional strain theory elements, that are superimposed on the shell element mesh used to model the cornea. The direction of the mesh edges automatically detects the orientation of the fibre sets. The mesh can be designed in such a way that it would capture two orthogonal fibre sets at the center and main circumferential fibre set at the corneal limbus as given in Figure 3.1.

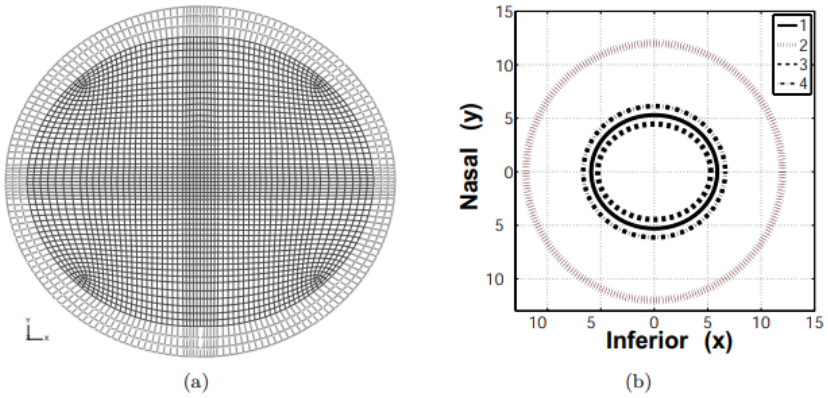

Figure 3.1: Reference configuration of the model, frontal view: (a) Mesh of the cornea — elements together with corneal limbus; (b) Eyeball: 1 – corneal profile, 2 – scleral profile, 3 – corneal limbus, 4 – scleral limbus

3.1 Loading Conditions

The ocular globe is filled with vitreous and aqueous humour and contains different structures such as focusing lens, iris and ciliary body. We are dealing with the IOP, which is, by definition, a tension exerted by the contents of the globe on the corneoscleral envelope. In the analysis, it is chosen to ignore all additional components inside the eye, assuming that they do not significantly affect the IOP. The eyeball was considered to be a cavity, filled with the vitreous and aqueous humour, which is represented as an incompressible gel-like substance. For the simulation of tonometry in 3D, it was essential to take this incompressibility into account:

boundary conditions should be stated with a constraint on the internal volume of the structure. In general, the response of the eyeball depends not only on the external loads but also on the pressure exerted by the intraocular fluid, which, in turn, is affected by the deformation of the structure. To analyse this situation the coupling between the deformation of the fluid-filled eyeball and the pressure from the contained fluid on the cavity boundary is needed. To ensure proper calculation of eye volume, all boundary edges are completely enclosed with hydrostatic fluid elements sharing the nodes with the boundary shell elements, which, in turn, consider transverse shear flexibility and membrane strains. A cavity reference node with a single degree of freedom representing the pressure inside was also defined on the intersection of the vertical symmetry axis and eyeball equator. It is adopted the notion that the eye is completely filled with incompressible fluid, which has the density of water at the body temperature, i.e. 994 kg/m^3. Later the density value would be varied to investigate the sensitivity of this parameter. Initially there is no contact between the tonometer tip and the eyeball. To prevent rigid body motion the optic nerve area was totally fixed during all the stages of the simulations. The tonometer head can be modelled with rigid solid elements. At the first preliminary step, the corneoscleral envelope was pressurized by prescribing special boundary conditions at the cavity reference node. This emulates the existence of IOP inside the eye and the fluid volume is automatically adjusted to fill the eyeball cavity after the step. At the next step, boundary condition was removed on the pressure degree of freedom, thus sealing the eye with the current fluid volume. In addition, contact was established between the tonometer and cornea. The final step was devoted to the GAT simulation, similar to 2D case. In the three-dimensional model, simulation of Goldmann tonometry was not limited to the central applanation, but extended to the paracentral application of the tonometer tip, implying the appearance of the error due to technique of procedure.

3.2 Numerical Details

In both 3D and 2D modelling, the incompressibility must be taken into consideration. In 3D this problem is avoided by employing conventional thin shell elements with $\nu = 0.5$ for the eyeball and hydrostatic fluid elements for the inside. The incompressibility of corneal material should be treated with care in 2D since continuum elements are used for the modelling. Due to the incompressibility of the material, the solution cannot be obtained in terms of the displacement history only, since a purely hydrostatic pressure can be added without changing the displacements. The material exhibits behaviour approaching the incompressibility limit: a small change in displacement produces very large changes in pressure. Therefore, a purely

displacement-based solution is too sensitive to be useful numerically. This difficulty is overcome by treating the pressure stress as an independently interpolated basic solution variable, coupled with the displacement solution through the constitutive theory and the compatibility condition. This independent interpolation of purely hydrostatic pressure is the basis of the hybrid continuum elements, specially designed for almost incompressible materials. Such hybrid elements are adopted for the simulations with axisymmetric models. Material nonlinearity was employed for both the cornea and the rebars and was implemented using a hyper elastic material model. It is described in terms of a strain energy potential, U(ε), which defines the strain energy stored in the material per unit of reference volume as a function of the strain at that point in the material. There are several forms of strain energy potentials available, as is a possibility to evaluate hyper elastic material behaviour with a particular U(ε) and compare with experimental test data. The experimental test data shall be evaluated to determine the optimal strain energy potential. It was found that the forms by Marlow and Van der Waals provided reasonable behaviour and the Marlow form of a strain energy potential can be adopted for all nonlinear constitutive relationships since it is found that this strain energy potential: (1) performs best in cases where limited sets of test data are available, and (2) is specially constructed to reproduce the test data exactly and showing a reasonable behaviour in other deformation modes, Hibbit *et al*. [8]. The conclusion is that second order reduced-integration hybrid elements perform best in 2D, while four-node doubly curved general purpose shell elements have satisfactory performance in 3D. These are adopted for the further simulations. To obtain accurate results, consideration must be given to the element size and mesh density selection. Our problems are geometrically nonlinear and for this type of analysis, in general, detailed convergence tests are required. However, present simulations are considering quasi-static dynamics; thus, it can be assumed that a simple two-density mesh monotonic convergence test is enough for the model verification. Several mesh densities are tested to achieve the optimal accuracy of the corneal mesh for both models. Non-linear axisymmetric and three-dimensional analyses has to be performed and the applanation force, required to achieve the needed area of contact is to be measured. The magnitude of this measured force is used as a quantity to express mesh convergence. The predictions are obtained using numerical models with quadrilateral axisymmetric elements and four-node shell elements, respectively. Initially, at the starting point of the simulation, no contact exists between the tip of the tonometer and the cornea and all the structures were assumed stress-free. Before the emulation of applanation tonometry, several preliminary steps were required.

In general, for any model, they are the following:

• IOP loading (15 or 21 mmHg);

• establishment of the contact between the GAT and cornea with the avoidance of rigid body motion;

• simulation of applanation tonometry and contact analysis between the anterior corneal surface and GAT tip. Deformation of the cornea by the tonometer proceeded until the contact area became 3.06 mm in diameter. At this area, full applanation is achieved and applanating pressure (IOPG) is calculated by dividing applanation force by the contact area.

Contact simulation is the third and the most important step in the analysis. The contact constraint enforcement method between the tonometer head and anterior corneal surface utilizes Lagrange multiplier degrees of freedom. This method uses a stiff approximation of hard contact as well as augmentation iterations to improve the accuracy of the approximation. The contact algorithm is based on the Newton-Raphson technique, which solves the nonlinear equations incrementally and iteratively by using the tangent stiffness matrix. It examines the state of all contact interactions at the start of each increment to establish whether master-slave gaps are open or closed. A constraint will be applied for each closed node and constraints are removed from any node where the contact state changes from closed to open. Equilibrium iteration is then carried out and the configuration of the model is updated using the calculated corrections. Before checking for equilibrium of forces or moments, any changes in the contact conditions at the slave nodes are checked. The contact constraints are modified to reflect the change in contact status between iterations. The procedure is repeated until the iteration is completed with no changes in contact status. This iteration becomes the first equilibrium iteration and the normal equilibrium convergence checks are performed. The entire process is repeated until convergence is achieved, Hibbit et al. [8].

3.3 Three-Dimensional Analysis [5]

Rebars rotate with the actual deformation and as a result of finite-strain effects they remain aligned with the element isoparametric directions. The adopted approach of modelling anisotropy with rebars has an advantage over modelling the same aspect with anisotropic material properties, since in the latter case under large shear deformation the anisotropic material directions initially aligned with the element isoparametric directions are determined based on the average rigid body rotation of the material point. The corneal tissue, thus, is

described as an anisotropic material, characterized by an isotropic matrix and two sets of reinforcing fibres, forming different angles in different locations of the cornea. The internal variables related to material performance correspond to separated contributions of the linear isotropic matrix and the hyper elastic rebars. To describe the behaviour of nonlinear generalised collagen fibrils, we needed to know the cross-sectional area of each rebar and their spacing in the plane of the shell. Knowing these parameters, we can describe the rebar reinforcement, which is treated as an additional equivalent layer smeared on the shell. The total corneal cross-sectional area $A = A_f + A_g$, where A_f and A_g are the areas of fibrils and ground substance in the cross-section, respectively. The area ratio is $A_f/(A_f + A_g) \approx 0.1$, which means that $A_f \approx 0.1A$. Only 66% of collagen fibrils are oriented, and calculating the cross-sectional area of the cornea (as a difference of integrals of the curves, describing anterior and posterior cornea surfaces), the total A_f of oriented rebars can be evaluated. Assuming the spacing between the rebars, $s = 0.1$ mm with known corneal geometry, the number of rebars is computed. Later, the corresponding area of each rebar, A_r, is also calculated as $A_r = 44 \times 10^{-4}$ mm^2. Young's modulus of the collagen fibrils in the fibril direction is of the order of 1.0 GPa, whereas Young's modulus of the ground substance is only of the order of 10−5 GPa. Collagen material is almost incompressible, and the cornea predominantly consists of water. Thus, Poisson's ratio for the isotropic matrix is 0.5.

Engineering stress-strain curves obtained from uniaxial tests on excised strips of the human corneas were fitted by an exponential function $\sigma = A(e^{B\varepsilon} - 1)$ using a least squares method. A tangential elastic modulus (E) was calculated as the gradient of the stress-strain relationship: $E \equiv E(\varepsilon) = d\sigma/d\varepsilon = A \times Be^{B\varepsilon}$. The test setup for the strip extensiometry is simple, with a cut cornea specimen attached to the grips of a tension machine and subjected to a gradually increasing axial tension. However, this technique is limited, mainly due to the cornea's initially curved surface. It is shown that at least some of the deficiencies are possible to overcome by applying more sophisticated post-processing procedures for deriving the material stress-strain relationship from test load extension data. Nevertheless, the previously reported studies adopt a simple straightforward procedure to determine constitutive material relationships:

$$\sigma = \frac{F}{A}, \quad A = wt, \quad \varepsilon = \frac{L - L_0}{L_0},$$

where F is an axial tension, A is the cross-sectional area of the specimen, w is the specimen width, t is the thickness and L_0 is the original length. In the first step, the specimen of the cornea is cut in the horizontal direction, as in Figure: 3.2.

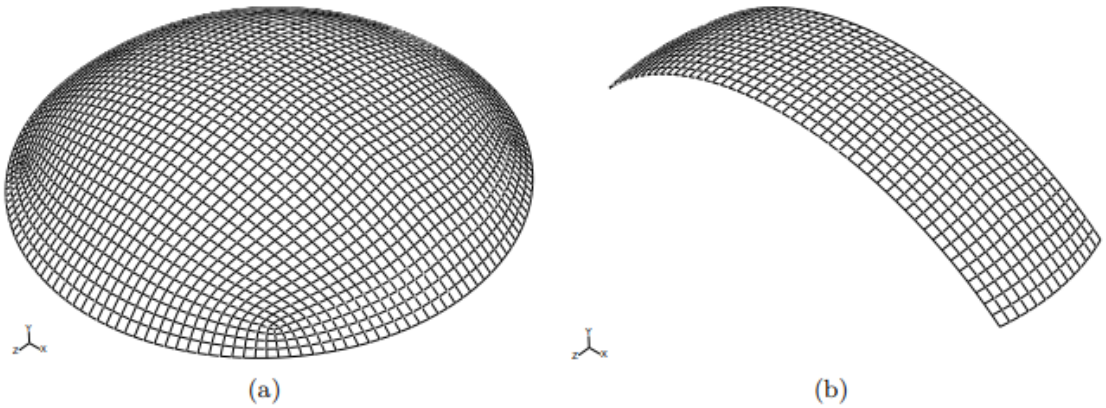

Figure 3.2: (a) Reference corneal configuration. Rebars are parallel to the edges of elements; (b) First step: cut the specimen of the cornea.

The procedure adopted in the numerical recreation of extensiometry tests closely follows the experimental set-up adopted by Wollensak *et al*. [9] with the width of the corneal strip equal to 3 mm. During the second step, a strip straightening can be performed. Usually, during the tests, some pre-stresses are applied to ensure that the strip is clamped horizontally before the application of the uniaxial force. Now simulate the corneal straightening using an analytical rigid surface pressing into the strip. At the end of the step, the strip takes a configuration shown in Figure: 3.3.

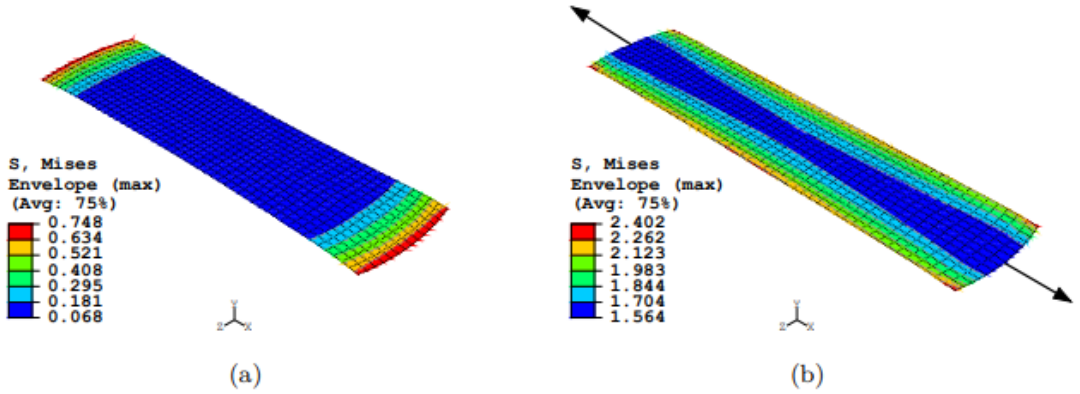

Figure 3.3: (a) Second step: straightening of the strip. Final configuration; (b) Third step: applying the uniaxial force. Final configuration. Contours are drawn on a model with material data from Wollensak *et al*. [9]. Those contours show the distribution of maximum von Mises stresses within the corneal strip

In the third step, all the nodes at both edges were constrained to have the same displacement in the x direction. The displacement of the middle nodes (arrows) is then prescribed to stretch. This technique allowed the total stretching force to be obtained directly as the reaction force at those nodes. All obtained data can be substituted into the above set of equations and the constitutive relationship for the rebars together with the elastic modulus of the ground matrix are derived in such a way that the stress-strain relationship closely fits the available after the proposed three steps.

Modelling of whole pressurized eye

The button inflation tests are considered to be more accurate than strip testing since the cornea is maintained in its natural condition and stress is bi-axial. The specimen includes the cornea and a narrow ring of surrounding scleral tissue, by which it is mounted on the test ring and subjected to a gradually increasing posterior pressure. The data related to the applied pressure and the corresponding apical displacement shall be monitored. Using mathematical analysis, the material constitutive relationship can then be derived. Figure: 3.4 shows five resulting pressure-apical curves obtained by Bryant & McDonnell [10] during their inflation tests.

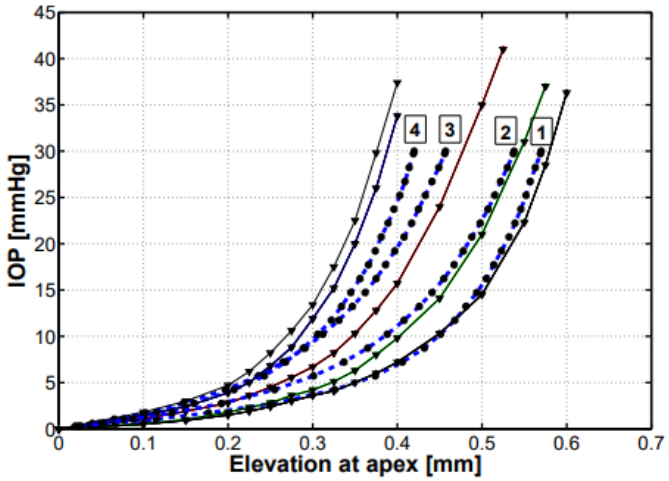

Figure 3.4: Pressure-displacement curves, obtained from five tests on pressurized eyes, Bryant & McDonnell [10]. They are shown with black solid lines. Fitted simulation results (curves $1-4$) are shown with the dotted lines, respectively

The dispersion of the data in this case can be explained by the difference in age and health conditions of the donors. The material model and the finite element mesh from Figure: 3.3(a) can be used to simulate experiments by Bryant & McDonnell [10]. Since no geometrical data are available in their article to differentiate the simulations; use standard corneal symmetric

geometry with R_c = 7.8 mm and D = 11 mm. During the simulations, all nodes at the limbus are constrained and the posterior corneal surface is loaded by a uniform pressure, progressively growing from 0 to 30 mmHg. Figure:3.4 contains pressure-displacement plots obtained by our numerical simulations. They are shown with the dotted lines and numbered (1 − 4). The curves of numerical data can be chosen to lie with a good correspondence between any experimental curves, depending on parameters A, B. Figure:3.4 shows nominal stress versus nominal strain exponential curves in form $\sigma = A(e^{B\varepsilon} - 1)$. These curves have been obtained from experimental data on corneal trephine inflation tests and fitted by an exponential function using a least squares method. Numerical simulations recreating those tests shall be performed and pressure-apical displacement curves can be obtained. Mathematical analysis based on the shell theory is utilized to study the behaviour of the corneal buttons. Both in-plane and out-of-plane stiffness components were considered, and it was assumed that the cornea could be approximated as a homogeneous spherical structure, Vito *et al*. [11].

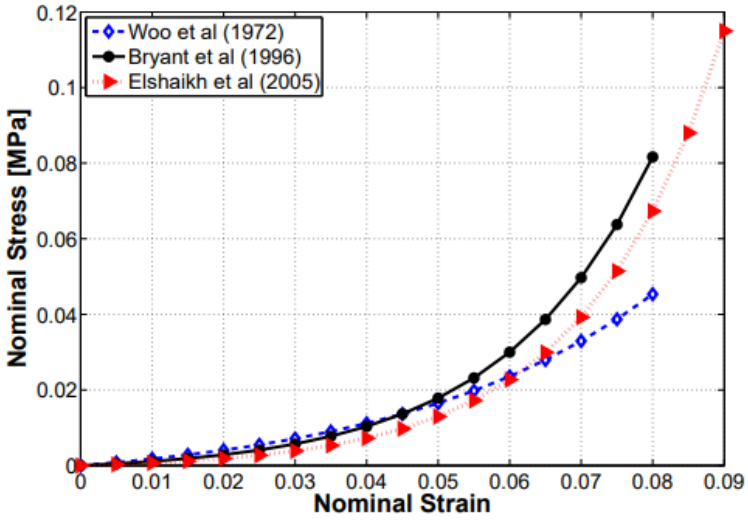

Figure 3.5: Constitutive relationship for the cornea, reported by Woo *et al*. [12]; Bryant & McDonnell [10]; Elsheikh & Anderson [7] during their inflation tests.

Equations to derive a constitutive relationship for the cornea from pressure-apical curves

After the pressure application, the corneal height, H, will increase by the apical rise recorded experimentally $H = H_0 + r$

The corresponding corneal radius is obtained from

$$R = \frac{1}{2H}\left[\left(\frac{D}{2}\right)^2 + H^2\right],$$

where D is the corneal base diameter. Assuming no change in the volume of material in the cornea after loading,

$$2\pi R_0 H_0 t_0 = 2\pi R H t.$$

Therefore, the new average thickness, t, is

$$t = \frac{R_0 H_0 t_0}{RH}$$

The half-central angle of curvature is

$$\theta = \sin^{-1}\left(\frac{D}{2R}\right).$$

The values of R, p, t and θ are then substituted into the final equation relating the internal pressure to the apical rise,

$$r = \frac{pR^2}{2Et}(1-\nu) - \frac{\nu R}{Et}\frac{pR}{2}(1-\nu)e^{-\beta\theta}\{\cos\beta\theta\},$$

where ν is a Poisson's ratio, taken as 0.5 based on the incompressibility assumption,

β = p (R/t) [3(1 − ν 2)]1/4. For each set of p − r data from (5.7), the corresponding modulus of elasticity, E, is derived. The meridian strain εϕ at this level of loading is then obtained using

$$\varepsilon_\varphi = \frac{1}{Et}(N_\varphi - \nu N_\theta),$$

where

$$\begin{cases} N_\varphi = \frac{pR}{2} \\ N_\theta = \frac{pR}{2} - \frac{pR}{2}(1-\nu)e^{-\beta\theta}\{\cos\beta\theta\}. \end{cases}$$

Therefore,

$$\varepsilon_\varphi = \frac{pR}{2Et}(1-\nu)(1+\nu e^{-\beta\theta}\cos\beta\theta)$$

The corresponding stress is then obtained using, σ = εE

The results from each of the numerical inflation tests are to be analysed using this procedure, giving a constitutive relationship for the cornea. Stress-strain relation in exponential form $\sigma_f = A_f (e^{Bf\varepsilon} - 1)$ as well as an elastic modulus of the embedded isotropic matrix are calibrated in order to ensure that the resulting corneal constitutive relationship matched the ones reported by Woo *et al*. [12]; Bryant & McDonnell [10]; Elsheikh & Anderson [7] and depicted in the above Figure 3.5.

3.4 Numerical study and Identification of the corneal tissue zones whose softening yielded keratoconus

A corneal numerical study was conducted by Falgayrettes *et. al* [13] to understand the biomechanics of keratoconus. The corneal dimensions used to construct the geometrical model were those of a healthy young author. They were measured *in vivo* with pachymetry and tomography and are central corneal thickness = 500 μm, peripheral corneal thickness = 620 μm, corneal height = 3.4mm, horizontal diameter = 11.8 mm, and vertical diameter = 10.7 mm. The author provided written informed consent to undergo the ophthalmological measurements and this study was approved by the Ethics Committee of the French Society of Ophthalmology. The corneal geometry was inserted into a piece of sclera to define smooth boundary conditions and avoid an unphysical cut. Since the cornea was linked to the sclera, the deformations were naturally transmitted in the 6 degrees of freedom. The sclera border was defined as fully blocked and the IOP loading was applied onto the internal surface of the cornea. The IOP used was that of the author whose corneal dimensions were used for the geometrical model (NF) (17.1 mmHg/2280 Pa).

They meshed the finite element model with 10-node quadratic tetrahedron elements and combined the material properties described above with the stroma-partitioned geometry. Since all the previous operations were conducted on the *in vivo* IOP deformed geometry, an inverse analysis working on the corneal geometry (nodes coordinates) was then run to determine the stress-free reference corneal dimensions (*i.e*. when the *in vivo* cornea was not subjected to IOP) with these particular boundary conditions and material properties. The stop criterion was reached when the reference geometry submitted to IOP matched the *in vivo* geometry previously recreated from the ophthalmological measurements. During this process, the solution was always computed with an implicit scheme in static analysis. The stress-free dimensions were: central corneal thickness = 550 μm, peripheral corneal thickness = 720 μm, corneal height = 2.9 mm, horizontal diameter = 11.8 mm, and vertical diameter = 10.7 mm. The stress-free thicknesses of the epithelium, Bowman's membrane, anterior, middle, and

posterior stroma, and Descemet's membrane plus endothelium in the center were 50, 10, 115, 166, 191, and 18 μm, respectively.

On this final model describing the five layers of the cornea in reference configuration and their material properties, they conducted a mesh convergence study to ensure that the mesh was fine enough to obtain accurate solutions and would not demand excessive computing resources. They conducted it by checking two variables that play key roles when the cornea is subjected to IOP, namely, vertical apex displacement and stress in the central anterior stroma. The solution reached convergence with a mesh of >40,000 elements.

The corneal elevation in keratoconus most often occurs in an inferocentral corneal button, which is softer and exhibits lamellar disorganization compared to the surrounding normal tissue. Therefore, first assessed whether gradually softening the collagen-based layers (*i.e*. Bowman's layer and stroma) in an inferocentral button in the corneal model geometry would generate keratoconus. For this, it has been added three concentric sections to the geometry, thus creating a button with a bullseye at the inferocentral cornea (Figure: 3.6a and 3.6b). Bowman's membrane and all stromal layers in the center, middle, and periphery of the button were then softened by dividing both their μ (ground-substance stiffness) and k1 (collagen-fibre stiffness) by 30, 20, and 10, respectively. This approach reduces stiffness in a linear pattern, as is typically seen in keratoconus. Normal IOP was then imposed. Softening the button effectively generated a keratoconic phenotype: the cornea bulged in an asymmetrical localized manner with a maximal vertical displacement of 846 μm (Figure: 3.6 d). By contrast, the normal cornea adopted a uniform curvature and maximal vertical displacement (U2) of 395 μm (Figure: 3.6c). The healthy (unsoftened) cornea is designated Case 1 while the 30-20-10 button softening condition is denoted Case 5. The keratoconic bulging in Case 5 was accompanied by increased thinning of the cornea: thus, imposition of normal IOP led the normal cornea to thin by 34 μm (from 550 to 516 μm) whereas the cornea with the weakened button thinned by 97 mm (from 550 to 453 μm) (Figure: 3.6c and 3.6d). The respective thicknesses of 516 and 453 μm for the healthy and keratoconic corneas are close to average minimum corneal thicknesses in the literature, namely, 537 μm in normal corneas and 436 (range 297–494) μm in keratoconus.

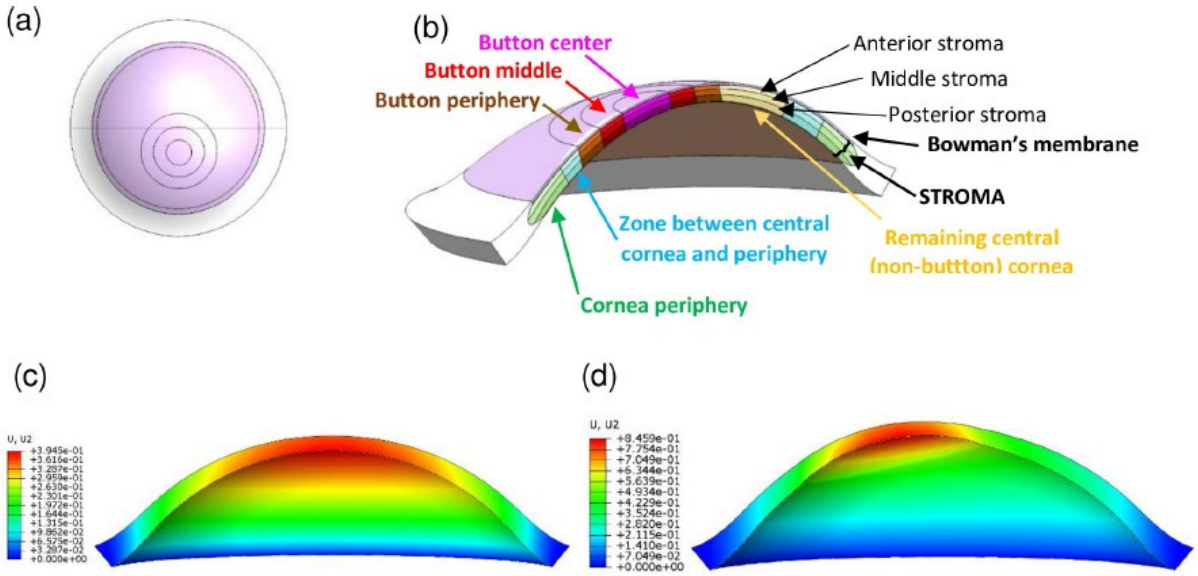

Figure 3.6: Generation of a softened button at the inferocentral zone of the model cornea (a, b) and its effect on vertical corneal displacement (U, U2, mm) (c, d). [13]

The keratoconic changes in Case 5 are also associated with the redistribution of the principal stress (which represents maximum tensional stress) on Bowman's membrane. Thus, in the healthy cornea, the tension spread evenly over the meridians and was regularly punctuated by concentric reinforcement stresses. By contrast, the keratoconic cornea exhibited a completely disrupted state of stress: tensional stress ran predominantly in latitudinal directions and was strong and highly disorganized at the inferocentral apex. It is notable that simply changing the stiffness of a button of tissue had such a radical effect on the tension throughout Bowman's membrane. Thus, our button model replicated the pathological corneal deformation and thinning that occurs in keratoconus. To further explore the mechanical stromal architecture-related mechanisms that underlie this disease, next it can be created four variant models: (1) examine the effect of milder button softening on corneal shape and thickness as a model of disease progression; (2) softened the entire cornea to determine whether a purely genetic condition can

create conical deformation; (3) softened specific corneal layers inside the button to determine how much mechanical support each layer contributes to cornea curvature; and (4) increased the dispersion of the posterior stromal lamellae in the button to determine whether simply altering this property could lead to keratoconus-like elevation.

4. PARAMETRIC ANALYSIS

All calculations are to be performed for two values of true IOP: 15 mmHg and 21 mmHg. The lower value has been chosen since it is a common value of IOP within young and healthy population, while a cut-off value of 21 mmHg has been widely used to differentiate between normal and abnormal IOP on statistical grounds. According to Darja Ljubimova [5], an extensive parametric study is necessary to evaluate the influence of biomechanical factors on the final results. Also, the behaviour of the models under the different loading cases of applanation is to be analysed.

4.1 Material Properties

One of the axisymmetric models represents a finite kinematics, nearly incompressible, linear orthotropic model to describe the mechanical response of stroma. In general, orthotropic materials are characterized by nine material engineering constants which are related to the stiffness of the tissue. Here, due to initial modelling assumptions, the number of independent parameters is reduced, since $\nu12 = \nu13$, $G12 = G13$ and $\nu23 = 0.5$ for all simulations. An extensive parametric study was performed to evaluate the influence of each six remaining material parameters, i.e., E1, E2, E3, ν12, G12, G23 on the performance of the model. It should be noted that due to the significant experimental data scatter and, sometimes, even the absence of meaningful ranges of data, the achievement of quantitative results was not the ultimate goal for the current numerical exercise. Present simulations were devoted to the observation of the behaviour pattern of the model, and the aim was to study the dependence of IOPG readings on the variation of one material parameter at a time, while the others were held constant. Thus, the most important outcome of the current parametric study is the sensitivity of IOPG measurements, not the IOPG values themselves. The transition in dominant stiffness from apex to limbus was included in the model. Pre-stresses were included in the model and before GAT application, cornea had represented a shell with in vivo geometric characteristics such as calibration geometry. A model with these reference material parameters, and calibration geometry obtained after application of IOPT, was adopted as the primal model for this parametric analysis. The sensitivity of resulting IOPG was determined from the baseline intraocular pressure values, calculated from this fundamental model. In the following we denote by E10, E20, E30 the adopted initial respective moduli average for all layers thorough the cornea thickness. Those would be used as markers at the x-axis showing variation of parameters span. E1, E2, G12 were related to the reference meridional modulus; thus, they

were to be expressed in terms of E30. Since some initial assumptions as well as modelling procedures can be called into question, all simulations were done with maximum possible ranges of parameter variations, in a manner that quantities were chosen 1) to meet initial assumptions and be comparable with values found in literature; 2) to meet the requirements of material stability and 3) to give successful numerical simulations without any unexpected abrupt stops and errors. Parametric simulations for each of the characteristic quantities have been performed and data points (calculated IOPG vs investigated parameter) were fitted to high-order polynomial functions, using a least squares procedure. Predicted span of results was obtained as well as IOPG variation per ±10% change of each variable from their respective baseline values. For the final estimation of the degree of influence of each parameter on model behaviour, the rate of IOPG change with respect to the independent quantity was calculated.

A) Elastic Radial Modulus — E1

E1 is the modulus of elasticity in the direction perpendicular to the corneal plane and its value is much smaller than the other elastic moduli. Initially, it was assumed to be 1% of the in-plane meridional modulus E30, which, in turn, had the same range of reported experimental values as the circumferential modulus E20. Simulations were carried out and E1 was varied, while other quantities were fixed at their baseline values. The relation between IOPG readings and variation of radial corneal modulus indicate rather complex behaviour. In order to investigate the influence of E1, it is divided the obtained distributions into two apparent regions, where IOPG values increased at different rates. According to the published sources, radial elastic modulus is equal to or, which is more likely, much smaller than elastic moduli in other directions due to the arrangement of collagen fibres in the cornea. Upper limit of $E1 = 5 \times E30$ is used for illustration purposes only to show the overall behaviour trend in the second region. One can observe that starting from the point when stiffness in corneal thickness direction is equal to stiffness in hoop direction the change in IOPG is nearly linear and rather small. The first proposed region is particularly interesting due to the fast change of IOPG measurements with parametric variation of E1. At first, the obtained data points within this region were fitted by a single nonlinear function. However, resulting curves did not approximate predictions with necessary accuracy.

B) Other Elastic Moduli — E2, E3

The first proposed region is particularly interesting due to the fast change of IOPG measurements with parametric variation of E1. At first, the obtained data points within this

region were fitted by a single nonlinear function. However, resulting curves did not approximate predictions with necessary accuracy. The effects of E2 and E3 alone were investigated independently, keeping the rest of material constants fixed. Resulting relationships for each modulus and consequent IOPG readings were fitted by nonlinear polynomial functions, separately. When average meridional modulus increases, IOPG measurements increases. In turn, with increasing value of average circumferential modulus IOPG readings decreases. Those two relationships are well approximated by second-degree polynomial functions

C) Poisson Ratios — ν12

This model operates within the linear elasticity theory, so $-1 \leq \nu12 \leq 0.5$. During the problem formulation, for simplicity, it is assumed that material was "almost transversally isotropic" in plane $2-3$. By that it is implied that Poisson's ratios and shear moduli obeyed the transversally isotropic law, but the elastic components were different, however not by much (i.e. $E20 = E30 - 0.1$ MPa). Also, for all layers $\nu12 = \nu13$. Taking into consideration the incompressibility of cornea as well as the fact that $\nu23 = 0.5$ and E1 being about two orders of magnitude smaller than E2 (or E3), the range of Poisson's ratios at which material stability requirements were fulfilled should be $|\nu12| \leq 0.05$. The adopted baseline value of $\nu120 = 0.01$. In further sensitivity study, consider only $\nu12 \geq 0$.

D) Transverse Shear Modulus — G12

In comparison with the elastic material data, not even a rough guide of possible magnitudes for the transverse shear corneal modulus was found in the literature. For simplicity, it is assumed that G12 = G13 for all layers thorough the cornea thickness. Reference value was adopted to be G120 = E30/5. Parametric simulations were carried out and the relationship between IOPG readings and variation of transversal shear corneal modulus was determined. Both upper and lower limits for the range of G12 were obtained: $G12 \geq E30/10$ — a condition for the existence of converged solutions and $G12 \leq 200 \times E30$ — a condition for avoidance of discontinuous jumps in contact pressure between the cornea and the tonometer tip. Similar behaviour pattern has been observed previously when the influence of elastic radial modulus E1 was investigated. For smaller parameter values the rate of IOPG change with respect to the independent quantity was more pronounced than for the larger parameter values. Although the overall trends of behaviour for G12 and E1 were similar, the actual alterations in IOPG were much smaller for a variation of G12 than for E1. To explore the effect of shear transverse modulus on the model

outcome, the same procedure as for E1 was utilized: the region was divided into two apparent parts (1, 2) depending on the rate of increase in IOPG predictions with increasing values of G12. In the first region G12 ∈ [E30/10; 25 × E30], while in the second G12 ∈ [25 × E30; 200 × E30]. Again, the relationship between shear transverse modulus and IOPG within the first proposed zone could not be approximated by only one high-order polynomial function with needed accuracy. Therefore, it is again divided the proposed region (1) into two parts (1a, 1b) and fitted them separately by different nonlinear curves. Within (1b) and (2) zones, the influence of G12 on predicted IOPG is nearly linea. Since G12 variation range is unknown, all three sub-regions are of interest. Overall influence on IOPG readings produced by this material constant alone is estimated to be around 4.5 mmHg with all adopted assumptions.

E) In-Plane Shear Modulus — G23

The baseline value for in-plane shear modulus G23 was chosen as 0.9 MPa. This parameter was varied quite extensively, from 0.001 MPa to 900 MPa. The observed difference in resulting IOPG during this simulation was within 1%, which was considered insignificant, with the conclusion that G23 variation does not significantly affect the results.

4.1 Variation of CCT

Simulations with both hyper elastic and orthotropic models were performed predicting for all material descriptions nonlinear relations between central corneal thickness (CCT) and IOPG readings. Measured variations of IOPG with CCT were fitted to the second-order polynomial. The adopted mean value of CCT of 537 μm was used to calculate the effect of CCT on the accuracy of GAT measurements, since the relationships were nonlinear. Here, on the x-axis of all the figures corneal thickness is the one measured in vivo. It is not the adopted initial thickness before simulation, but is the one after the application of IOP. The outcomes of four cases of orthotropic models were analysed, chosen specifically to investigate the material engineering constants of major influence on the results, as discussed above.

For the nonlinear isotropic material models the deviations of IOPG with thickness are larger than for the linear orthotropic models. Considering the outcome of simulations with isotropic hyper elastic corneas, one can observe that changes in IOPG predictions with thickness were the smallest for the models based on Elsheikh & Anderson [7].

5. CONCLUSIONS

Models in 2D and 3D are developed and a number of parametric simulations are conducted to study the accuracy of IOP predictions to the variation of each characteristic quantity. The resulting error estimates of IOPG associated with variability of each parameter are calculated, analysed and compared to the existing observations and previous theoretical studies. It is universally recognized that IOP depends on CCT. The identified correction factors are within the range reported by various manometric, population and theoretical studies. It is demonstrated that the effect of CCT is highly dependent on the corneal material properties. In fact, the influence of material parameters alone on IOPG seems to be larger than the influence of CCT on IOPG. A 2D axisymmetric linear heterogeneous orthotropic model is adopted to evaluate the effect of each biomechanical quantity on IOPG. The overall largest effects are produced by alterations in the elastic radial modulus E1, the meridional modulus E3 and the shear transverse modulus G12. Whereas it is apparent that magnitude of E1 is essential for the predicted IOPG, significant influence of meridional and shear transverse moduli is a new knowledge.

The 3D model of the cornea represents a nonlinear anisotropic composite structure with layering pattern of reinforcing collagen (two sets of families) parallel to the surface and embedded in a matrix of lower stiffness isotropic material. A finite element implementation is used to reproduce uniaxial tests on corneal samples and to simulate the mechanical behaviour of the whole cornea under the IOP loading. It is shown that with carefully chosen parameters, the proposed corneal material model is able to capture the uniaxial and inflation responses with good accuracy. This illustrates the good performance of the model and the physical mechanisms that are inherited by the constitutive model. The ability of the model to reproduce the behaviour of human cornea, despite large experimental dispersion opens a promising perspective for the future numerical simulations. In 2D, the assumption of linearity of constitutive corneal model seems to be insufficient to capture all the aspects of corneal behaviour under the application of IOP. Nevertheless, this is done to study the behaviour pattern of IOPG dependence on the variation of each of orthotropic material constants.

The proposed numerical models are valuable to the scientific community, since they can be used as tools for suggesting the magnitudes of the influences of corneal biomechanics. Any of these two parameters have a potential to affect IOPG to a higher degree than variation in CCT. The important new knowledge is the introduction of the modelling procedures that incorporate

the synthesis of disparate sets of geometric and mechanical data from a variety of published sources. Numerically recreated experimental tests accurately capture mechanical behaviour of the tissue and are used to derive material laws for the unknown parameters (i.e. ground substance and embedded rebars) for further utilization in GAT simulations. Different configurations of the structural model can easily be simulated by appropriate adjustments of parameters. The reported modelling exercises serve as a platform for understanding the biomechanics of the normal corneal tissue. After careful validation against experimental data, established FE models can be extended on the tissues, deformed by disease or any kind of surgery. In turn, a full comprehension of biomechanical processes in the cornea leads to better insight about the dependencies of predicted IOPG from various properties, particularly, in pursuit of necessary corrections required to achieve accurate IOPG readings. In general, it is believed that all introduced models show rather predictable, reasonable behaviours, which are favourably consistent with different published data. Thus, the proposed numerical procedure is certainly useful in its present form.

References

[1] www.ma.utexas.edu

[2] http://www.onset.unsw.edu.au

[3] Young L Kim, Joseph T Walsh Jr, Thomas K Goldstick & Matthew R Glucksberg (2004), Variation of corneal refractive index with hydration; *Physics in Medicine & Biology (IOP)*, Volume 49 (5)

[4] Umberto Lucia, Giulia Grisolia, Sabrina Francia, Maria Rosa Astori & Antonio Ponzetto (2016), Constructal approach to bioengineering: the ocular anterior chamber temperature*; Nature (Scientific reports)*

[5] Darja Ljubimova, Biomechanics of the Human Eye and Intraocular Pressure Measurements, *Doctoral thesis* (2009), Department of Mechanics, Royal Institute of Technology, Sweden.

[6] Hamed Hatami-Marbini & Md Esharuzzaman Emu; Effect of corneal collagen crosslinking on viscoelastic shear properties of the cornea, *Journal of the mechanical behavior of biomedical materials* 133 (2022) 105300

[7] Elsheikh, A. & Anderson, K. (2005); Comparative study of corneal strip extensometry and inflation tests, *Journal of the Royal Society Interface* 2(3), 177-185.

[8] Hibbit, Karlsson & Sorensen (2004); *ABAQUS Documentation 6.5-6*. Pilgatan 8c, SE-721 30 Vasteras, Sweden: ABAQUS Scandinavia AB.

[9] Wollensak, G., Spoerl, E. & Seiler, T (2003); Stress-strain measurements of human and porcine corneas after riboavin-ultraviolet-A-induced cross-linking. *Journal of Cataract and Refractive Surgery* 29(9), 1780-1785.

[10] Bryant, M. R. & McDonnell, P. J. (1996); Constitutive laws for biomechanical modelling of refractive surgery. *Journal of Biomechanical Engineering* 118(4), 473-481.

[11] Vito, R. P., Shin, T. J. & McCarey, B. E. (1989); A mechanical model of the cornea: The effects of physiological and surgical factors on radial keratotomy surgery. *Refractive and Corneal Surgery* 5(2), 82-88.

[12] Woo, S. L., Kobayashi, A. S., Schlegel, W. A. & Lawrence, C. (1972) Nonlinear material properties of intact cornea and sclera. *Experimental Eye Research* 14(1), 29-39.

[13] Falgayrettes N, Patoor E, Cleymand F, Zevering Y, Perone J-M (2023) Biomechanics of keratoconus: Two numerical studies. *PLoS ONE* 18(2): e0278455.